

**Title Page**

**Title:** A Receptor Tyrosine Kinase Network Comprised of FGFRs, EGFR, ERBB2 and MET Drives Growth and Survival of Head and Neck Squamous Carcinoma Cell Lines

**Authors:** Katherine R. Singleton, Jihye Kim, Trista K. Hinz, Lindsay A. Marek, Matias Casás-Selves, Clark Hatheway, Aik Choon Tan, James DeGregori, and Lynn E. Heasley

**Affiliations:** Departments of Craniofacial Biology (K.R.S., T.K.H., L.A.M., C.H., L.E.H.), Medicine (J.K., A.T.), and Biochemistry and Molecular Genetics (M.C.S., J.D.), University of Colorado Anschutz Medical Campus, Aurora, Colorado 80045

**Running Title Page**

**Running Title:** Synthetic lethal relations identify a RTK network in HNSCC

**Corresponding Author:** Katherine R. Singleton

Department of Craniofacial Biology

School of Dental Medicine, University of Colorado Anschutz

Medical Campus

Mail Stop 8120, P.O. Box 6511, Aurora, CO 80045

Email: katherine.singleton@ucdenver.edu

**Number of Pages:** Text – 21 pages (not including figure legends)

Tables – 0 + 2 Supplemental Tables

Figures – 7 + 6 Supplemental Figures

References – 49

**Number of Words:** Abstract – 248

Introduction – 747

Discussion – 923

**List of Non-Standard Abbreviations:**

AKT – protein kinase B

ALK – anaplastic lymphoma kinase

BiNGS! - Bioinformatics for Next Generation Sequencing

BSA – bovine serum albumin

CML – chronic myeloid leukemia

DMEM – Dulbecco's modified Eagle medium

DMSO – dimethyl sulfoxide

EGFR - epidermal growth factor receptor

EPHB2 – ephrin receptor B2

ERBB2 - epidermal growth factor receptor 2

ERK – extracellular signal regulated kinase

ESCC – esophageal squamous cell carcinoma

FBS – fetal bovine serum

FDR – false discovery rate

FGF2 – fibroblast growth factor 2

FGFR - fibroblast growth factor receptor

FZD – frizzled

HGF – hepatocyte growth factor

HNSCC - head and neck squamous cell carcinoma

INSRR – insulin receptor related receptor

JAK – Janus kinase

MAPK – mitogen-activated protein kinase

MEK2 – mitogen activated protein kinase kinase 2

MET- hepatocyte growth factor receptor

MOI – multiplicity of infection

NB – negative binomial

NSCLC – non-small cell lung cancer

p16<sup>INK4A</sup> – cyclin-dependent kinase inhibitor 2A

p53 – tumor protein 53

PARP – poly ADP ribose polymerase

PBS – phosphate buffered saline

PI3K – phosphoinositide 3-kinase

PTEN – phosphatase and tensin homolog

PTK7 – protein tyrosine kinase 7

RAS – rat sarcoma

Rb – retinoblastoma protein

RPMI-1640 – Roswell Park Memorial Institute-1640

RTK - receptor tyrosine kinase

SDS – sodium dodecyl sulfate

SHP2 – tyrosine-protein phosphatase non-receptor type 11

SLAT - synthetic lethal with AZ8010 treatment

SOS2 – son of sevenless 2

STAT - signal transducer and activator of translation

TCF7 – T-cell factor

TKI - tyrosine kinase inhibitor

TNKS – tankyrase

TTBS – Tris-buffered saline with 0.1% Tween 20

**Abstract:**

Our lab has previously shown that some gefitinib insensitive head and neck squamous cell carcinoma (HNSCC) cell lines exhibit dominant autocrine fibroblast growth factor receptor (FGFR) signaling. Herein, we deployed a whole genome loss-of-function screen to identify genes whose knockdown potentiated the inhibitory effect of the FGFR inhibitor, AZ8010, in HNSCC cell lines. Three HNSCC cell lines expressing a genome-wide shRNA library were treated with AZ8010 and the abundance of shRNA sequences was assessed by deep sequencing. Underrepresented shRNAs in treated cells are expected to target genes important for survival with AZ8010 treatment. Synthetic lethal hits were validated with specific inhibitors and independent shRNAs. We found that multiple alternate receptors provided protection from FGFR inhibition, including receptor tyrosine kinases (RTKs), epidermal growth factor receptor 2 (ERBB2) and hepatocyte growth factor receptor (MET). We showed that specific knockdown of either ERBB2 or MET in combination with FGFR inhibition led to increased inhibition of growth relative to FGFR tyrosine kinase inhibitor (TKI) treatment alone. These results were confirmed using specific small molecule inhibitors of either ERBB family members or MET. Moreover, the triple combination of FGFR, MET and ERBB family inhibitors showed the largest inhibition of growth and induction of apoptosis as compared to the double combinations. These results reveal a role for alternate RTKs in maintaining pro-growth and survival signaling in HNSCC cells in the setting of FGFR inhibition. Thus, improved therapies for HNSCC patients could involve rationally designed combinations of TKIs targeting FGFR, ERBB family members and MET.

## **Introduction:**

Over 500,000 patients worldwide are diagnosed with HNSCC yearly. With a 5-year survival of only 50% (Haddad et al., 2008), HNSCC exhibits one of the poorest survival rates among common cancer types. Therapy for HNSCC has seen little advancement in recent years and largely involves improved chemotherapy schedules and use of intensity-modulated radiation (Murdoch 2007). Unlike other cancers, the frequency of oncogenic driver mutations (Agrawal et al., 2011; Stransky et al., 2011) in HNSCC is low. Rather, HNSCC tumors are characterized by mutations in tumor suppressors such as tumor protein 53 (p53), cyclin-dependent kinase inhibitor 2A (p16<sup>Ink4A</sup>), phosphatase and tensin homolog (PTEN) and retinoblastoma protein (Rb) (reviewed in (Leemans et al., 2011)). Approximately 90% of HNSCC tumors overexpress epidermal growth factor receptor (EGFR) (Dassonville et al., 1993) and EGFR ligands, correlating with poor prognosis (Dassonville et al., 1993; Grandis et al., 1996; Grandis et al., 1998; Ang et al., 2004). From this evidence, trials of the EGFR TKIs, gefitinib and erlotinib, and the inhibitory antibody, cetuximab, were completed in HNSCC patients. While no significant response to EGFR TKIs was observed, cetuximab yielded a modest increase in survival (Cohen et al., 2003; Soulieres et al., 2004; Cohen 2006; Specenier et al., 2011) and is approved for HNSCC treatment (Specenier et al., 2011).

The hypothesis that tumor heterogeneity across a cancer type dictates therapeutic response forms the basis of personalized medicine and shows promise for improved treatment of non-small cell lung cancer (NSCLC). In trials of NSCLC patients treated with an EGFR TKI, responses are limited to tumors bearing EGFR mutations

(Shepherd et al., 2005; Gazdar 2009). However, EGFR mutations are rare in HNSCC (Agrawal et al., 2011; Stransky et al., 2011) and attempts to match EGFR expression or gene copy number with cetuximab response have failed (Egloff et al., 2009; Licitra et al., 2011). Recently, we showed that a possible intrinsic resistance mechanism of HNSCC cells to EGFR inhibition is mediated by an RTK autocrine loop comprised of FGFRs and fibroblast growth factor 2 (FGF2) that could be inhibited with FGFR TKIs (Marshall et al., 2011). This work highlighted an FGFR autocrine loop as a novel target for improved HNSCC therapy and illustrated how growth of tumors may be driven distinct from traditional oncogenic mutations.

Evidence supports the activity of other alternate RTKs in growth of HNSCC. ERBB2 is a dominant mediator of growth in a subset of breast cancers (Perou et al., 2000). Also, ERBB2 is amplified in esophageal squamous cell carcinomas (ESCCs) and overexpression is linked to lowered survival (Sato-Kuwabara et al., 2009). ERBB2 is overexpressed in 20-40% of HNSCC tumors with gene amplification in 5-10% of cases, correlating with decreased survival (reviewed in (Morgan et al., 2009)). A role for an additional RTK, MET, is emerging in HNSCC. MET is overexpressed in some HNSCC tumors and efficacy of MET TKIs to reduce survival and migration of HNSCC cells has been shown (Seiwert et al., 2009). However, the full role of this RTK in the survival of HNSCC cells remains uncertain.

Following the success of the ABL inhibitor, imatinib mesylate, in the treatment of BCR-ABL-positive chronic myeloid leukemia (CML) (Druker 2002), cancer research has increasingly focused on identifying and targeting similar driver events in other cancers (Stambuk et al., 2010). The success of imatinib lies primarily in BCR-ABL being the sole

driving event for CML (Druker 2002), but other cancers have not proven as tractable. NSCLC is not characterized by a single driver, but by many, resulting in the need for patient stratification before treatment (Ladanyi et al., 2008). Some drivers are difficult to identify, as illustrated by the response of HNSCC patients to EGFR inhibitors (Kalyankrishna et al., 2006) while others, exemplified by RAS, remain difficult to target (Hopkins et al., 2002). In addition, even with targeted therapy, a significant number of patients will develop resistance (O'Dwyer et al., 2004). As a result, attention has focused on discovering biomarkers for patient selection as well as exploring novel combination therapies (Morse et al., 2010). With this goal, we performed a genome-wide shRNA loss-of-function screen to identify targets whose inhibition would improve the response of HNSCC cells to FGFR TKIs. We found that HNSCC cell lines rely on the activation of multiple alternate RTKs, including ERBB2 and MET, to fully establish growth and survival. Our findings are consistent with the hypothesis of RTK coactivation (Xu et al., 2010) and responds to a call for development of therapies comprised of combinations of targeted inhibitors (Glickman et al., 2012).



## **Materials and Methods:**

**Cell Culture:** All HNSCC cell lines used in this study were submitted to fingerprint analysis by the University of Colorado Cancer Center DNA Sequencing and Analysis Core confirming their authenticity. Cell lines were routinely cultured in Dulbecco's modified Eagle medium (DMEM) or Roswell Park Memorial Institute-1640 (RPMI-1640) (584-A2, MSK-921) growth medium (Invitrogen, Carlsbad, CA) supplemented with 10% fetal bovine serum (FBS) with 1% penicillin-streptomycin (Sigma-Aldrich, St. Louis, MO) at 37°C in a humidified 5% CO<sub>2</sub> incubator.

**Lentivirus Preparation:** The HIV based GeneNet Lentiviral Human 50K library (pSIH1-H1-Puro, System Biosciences, SBI, Mountain View, CA) was packaged in 293T cells with packaging component vectors coding for VSV-G, Gag, Pol, and Rev (generously provided by Dr. Douglas Graham, Dept. Pediatrics, UC Denver Anschutz Medical Campus). Cells were incubated overnight with Turbofect transfection reagent (Fermentas, Glen Burnie, MD), packaging vectors and library. The lentiviruses released into the medium were filtered using a 0.45 µm filter (Corning Inc., Corning, NY). 4x10<sup>6</sup> cells from each of the cells lines UMSCC25, 584-A2, and CCL30 were plated and transduced 24 hrs later with the SBI shRNA library containing viral media and 8 µg/mL polybrene (Sigma-Aldrich) at a multiplicity of infection (MOI) of ~0.2. Viral titer was determined by serial dilution. After 72 hrs, transfected cells were selected with puromycin (1 µg/mL) for 5 days. For validation of synthetic lethal hits, five independent

shRNAs (Supplemental Table 1) in the lentiviral vector pLKO.1 and the pCMV-VSV-G and pΔ8.9 packaging component vectors were obtained from the Functional Genomics Facility at the University of Colorado at Boulder. All cultures were confirmed for knock down and submitted to growth assays within three passages of puromycin (1 μg/mL, Sigma-Aldrich) selection.

**Genome-Wide RNAi-Based Functional Screening:** Library expressing HNSCC cells were divided into six groups of  $5 \times 10^6$  cells per T-75 flask (BD Biosciences, Franklin Lakes, NJ), where three were treated with vehicle (dimethyl sulfoxide, DMSO) and three groups were treated with AZ8010 (1.0 μM for UMSCC25, 0.125 μM for 584-A2 and 0.5 μM for CCL30). After 72 hrs, the cells were placed in media without drug for an additional 72 hrs. Total RNA was purified from each replicate using an RNeasy Mini Kit (Qiagen, Germantown, MD) and reverse transcribed using vector specific primers (SBI) and MMLV reverse transcriptase (Invitrogen, Carlsbad, CA). The cDNA was amplified using nested PCR to isolate the shRNA sequences and to add Illumina adapter sequences. The samples were sequenced on an Illumina Genome Analyzer IIx (Illumina, San Diego, CA).

**Bioinformatics Analysis:** To analyze and interpret the sequence data obtained from the Genome Analyzer, we used the bioinformatics pipeline, BiNGS! (Bioinformatics for Next Generation Sequencing) (Kim et al., 2012), as described and validated in previous studies (Casas-Selves et al., 2012; Porter et al., 2012; Sullivan et al., 2012). Briefly, after filtering steps, Negative Binomial (NB) was then used to model the distribution of

read counts of the data using edgeR (Robinson et al., 2007). The q-value of the false discovery rate (FDR) was calculated for multiple comparisons. In order to combine multiple shRNAs into genes, we adapted weighted Z-transformation. It is based on the product of q-value, which follows a chi-square distribution with  $2k$  degrees of freedom (where  $k$  is the number of p-values) (Whitlock 2005). Lists of genes with differentially represented shRNAs were ranked using the associated p-value  $[P(wZ)]$ . By multiplying the  $P(wZ)$  value by the rank of the gene, an E-value was obtained. E-value is an estimation of false positivity. The resulting data sets have been deposited in NCBI GEO Database (Accession #GSE39305)

**Clonogenic Growth Assay:** To measure the effect of inhibitors or shRNA-mediated knock down on cell growth, cells were seeded at 100 cells per well in six well tissue culture plates in full media. After 24 hrs, cells were treated as indicated and cultured for 14 days with the addition of fresh media containing inhibitors every 7 days. Plates were rinsed twice with phosphate buffered saline (PBS) and fixed and stained with 0.5% (wt/vol) crystal violet in 6.0% (vol/vol) gluteraldehyde solution for 30 min at room temperature. Plates were rinsed in distilled  $H_2O$  and photographed. The MetaMorph imaging software program (Molecular Devices, Downingtown, PA) was used to quantify total colony area.

**Anchorage-Independent Growth Assay:** In order to measure the effect of inhibitors on anchorage independent growth, 20,000 cells were suspended in 1.5 mL of growth media containing 0.35% Difco agar noble (Becton, Dickinson and Co., Franklin Lakes,

NJ) and overlaid on a base layer of growth media containing 0.5% agar noble. Drugs were added by overlay with 2 mL growth media. Media and drugs were replaced once a week. After 14 days, plates were stained for 24 hrs with 200  $\mu$ L of 1 mg/mL nitroblue tetrazolium and photographed. MetaMorph was used to quantify total colony number.

**Cell Proliferation Assay:** Cells were plated at 50 cells per well in either 96 or 48 well tissue culture plates and treated with inhibitors at various doses. After the DMSO-treated control wells had become confluent (1-2 weeks), cell numbers were assessed using a CyQUANT Direct Cell Proliferation Assay (Invitrogen) according to the manufacturer's instructions.

**Immunoblot Analysis:** Phospho-extracellular signal regulated kinase (ERK), phospho-MET, phospho-AKT, phospho-ERBB2, phospho-EGFR, phospho-STAT3, poly ADP ribose polymerase (PARP) and caspase-3 levels in HNSCC cells were measured by immunoblotting. Cells in 10 cm tissue culture dishes were treated with different inhibitors in full growth media. After treatment, cells were rinsed once in PBS, collected in PBS and centrifuged at 2,000 x g for 3 min. The cell pellet was lysed in buffer containing 0.5% Triton X-100, 50 mM  $\beta$ -glycerophosphate (pH 7.2), 0.1 mM  $\text{Na}_3\text{VO}_4$ , 2 mM  $\text{MgCl}_2$ , 1 mM EGTA, 1mM DTT, 0.3 M NaCl, 2  $\mu$ g/mL leupeptin and 4  $\mu$ g/mL aprotinin. Samples were centrifuged at 13,000 x g for 5 min and the particulate fraction was discarded. Aliquots of cell extracts were added to 25  $\mu$ L of sodium dodecyl sulfate (SDS) loading buffer and proteins were resolved by SDS-PAGE. After electrophoretic transfer to nitrocellulose, filters were blocked in 3% bovine serum albumin (BSA; Cohn

Fraction V, ICN Biomedicals, Inc., Aurora, OH) in Tris-buffered saline with 0.1% Tween 20 (TTBS). The filters were then incubated overnight at 4°C with anti-phospho-Erk, phospho-MET (Tyr1234/1235), phospho-Akt (Thr308), phospho-ERBB2 (Tyr1248), phospho-STAT3 (Ser727) (Tyr705), PARP or caspase-3 (Cell Signaling Technology, Inc., Danvers, MA, #9101, #3077, #4056, #2247, #3281, #9134, #9145, #9542 and #9661) The filters were washed three times in TTBS and incubated for one hour at room temperature with alkaline phosphatase coupled goat anti-rabbit antibodies. The filters were developed using LumiPhos reagent (Pierce, Rockford, IL) according to the manufacturer's instructions. The filters were stripped and reprobed for total ERK1 and 2 or Na/K-ATPase using a mixture of ERK1 and ERK2 antibodies or Na/K-ATPase  $\alpha$ -subunit antibodies (Santa Cruz Biotechnology, Inc., Santa Cruz, CA, sc-93, sc-154 and sc-21712). The filters were also reprobed for total MET, total AKT, total STAT3, total ERBB2 and total EGFR (Cell Signaling Technology, Inc., #3127, #9272, #9132, #2242 and #2232).

**Caspase 3 Activity Assay:** Caspase 3 activity was assessed as previously described (Matassa et al., 2001).

**Chemicals:** AZ8010 and AZD8931 were obtained by Material Transfer Agreements from AstraZeneca (Wilmington, DE). PF02341066 and lapatinib were obtained from Selleck Chemicals (Houston, TX).

## **Results:**

**A synthetic lethal screen identifies genes whose silencing enhances growth inhibition by FGFR-specific TKIs.** In order to identify targets whose inhibition would sensitize HNSCC cells to FGFR TKIs, three cell lines expressing a genome-wide library of shRNAs were used in a loss-of-function screen (Fig. 1A). The HNSCC cell lines used to express the shRNA library were UMSCC25 and 584-A2, cell lines derived from tumors of the larynx, and CCL30, derived from a tumor of the nasal septum. UMSCC25 cells are highly dependent on EGFR for growth and signaling while FGFRs function as an auxiliary growth pathway (Supplemental Figure 1A and (Marshall et al., 2011)). By contrast, CCL30 and 584-A2 cells are dependent on FGFR alone for growth as evidenced by high sensitivity to treatment with the FGFR specific TKI, AZ8010 (Supplemental Figure 1A and B, (Marshall et al., 2011)). The levels of EGFR and FGFRs in these cell lines were published previously (Marshall et al., 2011).

Cell lines stably expressing the lentiviral shRNA library with the majority of cells expressing only one shRNA were treated with DMSO for 72 hours followed by 72 hours of recovery in drug free media. Alternatively, the cell lines were treated with the FGFR inhibitor, AZ8010, for 72 hours at concentrations that reduced growth by approximately 30% as compared to DMSO treated controls, followed by a 72 hour recovery period without drug. Total RNA was then isolated from each treatment group, and the shRNAs were amplified, sequenced and analyzed as described in the Materials and Methods. Nearly 28 million reads were generated for each replicate and the reads were found to cluster within treatment groups and cell lines via unsupervised hierarchical clustering (Supplemental Figure 2). This indicates that the drug treatment is reproducibly affecting

the proportions of shRNAs present in the cell populations and that the knockdown of certain genes can modulate the response of cells to AZ8010 treatment.

In order to consider a gene a synthetic lethal with FGFR inhibition, we chose an E value  $\leq 2$  as the cut-off (Supplemental Table 2) from the BiNGS! ranked genes. We termed the synthetic lethal hits Synthetic Lethal with AZ8010 Treatment (SLAT) and detected 504 SLATs in UMSCC25 cells, 292 SLATs in 584-A2 cells, and 104 SLATs in CCL30 cells. While there was varying amounts of overlap between any two cell lines, with UMSCC25 and 584-A2 sharing the most SLATs (25), CCL30 sharing 9 with UMSCC25 and 9 with 584-A2, there were no SLATs observed in common among all three cell lines (Supplemental Figure 3). This likely reflects the distinct differences in growth drivers between 584-A2 and CCL30 cells (FGFR dominant) and UMSCC25 cells (EGFR dominant).

For the remainder of the study, we have chosen to focus on the SLATs identified in UMSCC25 cells that support a RTK network comprised of FGFRs, EGFR, ERBB2 and MET as the functional growth pathway. Where relevant, we use the functional genomics data from 584-A2 and CCL30 to highlight why ERBB2 and MET were not identified as SLATs in these cell lines. The ten highest ranking SLATs identified in UMSCC25 cells are shown in Figure 1B with the raw sequencing counts in triplicate for each shRNA indicated. Notably, the RTK, *MET*, was identified as a SLAT based on three distinct shRNAs, while *ERBB2* was identified based on a single shRNA. While no synthetic lethal genes were observed in common among the three cell lines, there were receptor tyrosine kinases, G-protein coupled receptors and specific downstream signaling components identified as SLATs in all the lines. For example, the insulin

receptor related receptor (INSRR) and the ephrin receptor B2 (EPHB2) were identified as highly ranked SLATs in 584-A2 and protein tyrosine kinase 7 (PTK7) and the Wnt/Frizzled (FZD) pair, WNT16 and FZD7, were identified in CCL30 cells. Moreover, genes encoding signaling enzymes associated with WNT signaling (T-cell factor (TCF7) and tankyrase (TNKS)), phosphoinositide 3-kinase (PI3K) signaling (PIK3C3, PIK3R2, PIK3CB and AKT2), Janus kinase-signal transducer and activator of translation (JAK-STAT) signaling (STAT1 and STAT2), RAS/ERK signaling (son of sevenless 2 (SOS2), KRAS, tyrosine-protein phosphatase non-receptor type 11 (SHP2) and mitogen activated protein kinase kinase 2 (MEK2)) were identified as SLATs with a less stringent cut off of E value  $\leq 20$ , which still corresponds to a p value  $\leq 0.05$  (Fig. 1C). Overall, the results from the synthetic lethal screen support the hypothesis of “RTK coactivation”, whereby cancer cells rely on activation of multiple RTKs to maintain flexible and vigorous signaling responses in the face of various insults such as drug treatment (reviewed in (Xu et al., 2010)). To investigate whether HNSCC cell lines maintain growth in this manner, we have focused the remainder of the study on UMSCC25 cells and validation and further exploration of the SLATs, ERBB2 and MET.

**Validation of ERBB2 and MET as synthetic lethal genes with FGFR-specific TKIs in UMSCC25 cells.** Both ERBB2 and MET are broadly expressed in a panel of HNSCC cell lines including UMSCC25 cells (Figure 2). It is noteworthy that the FGFR dependent cell lines, 584-A2 and CCL30, express reduced levels of ERBB2 and MET, respectively, and neither of these RTKs were identified as SLATs in these cell lines in the initial screen. ERBB2 is a ligand independent member of the EGFR family that heterodimerizes with other members of the ERBB family to initiate downstream



signaling to mitogen-activated protein kinase (MAPK), protein kinase B (AKT) and JAK-STAT pathways (reviewed in (Hynes et al., 2005)). MET is a RTK, where, upon binding of the receptor's ligand, hepatocyte growth factor (HGF), MET is phosphorylated and participates in signaling for survival, motility and proliferation (reviewed in (Cecchi et al., 2010)). To validate ERBB2 and MET, UMSCC25 cells were transduced with two independent shRNAs targeting ERBB2 and two independent shRNAs targeting MET. The shRNAs were from the TRC library, distinct from those used in the original screen, and the level of target knockdown was determined by immunoblot (Fig. 3A). Consistent with the screen results, the combination of AZ8010 treatment and ERBB2 knockdown resulted in greater growth inhibition as compared to either treatment alone (Fig. 3B). Similarly, MET knockdown alone decreased clonogenic growth of UMSCC25 cells relative to the non-silencing control construct (NSC) expressing UMSCC25 cells. Additionally, confirming the screen results, knockdown of MET in combination with FGFR inhibition caused a greater reduction of clonogenic growth than AZ8010 treatment or MET knockdown alone (Fig. 3C). These data provide molecular validation of ERBB2 and MET as being synthetic lethal with an FGFR inhibitor in UMSCC25 cells.

**A pan-ERBB inhibitor, AZD8931, yields synergistic inhibition of proliferation with FGFR-specific TKIs.** Because genetic knockdown of ERBB2 sensitizes UMSCC25 cells to AZ8010 treatment, we investigated whether pharmacological inhibitors of the ERBB family have a similar effect. The small molecule TKI, AZD8931, is a reversible, equipotent inhibitor of the ERBB family members EGFR, ERBB2 and ERBB3 and has been shown to have significant anti-growth effects in NSCLC and HNSCC xenografts in mice (Hickinson et al., 2010). AZD8931 potently

inhibited tyrosine phosphorylation of ERBB2 and EGFR in UMSCC25 cells, consistent with published results in other cell lines (Supplemental Figure 4A and B). UMSCC25 cells, in which ERBB2 was identified as a SLAT, showed a significant decrease in growth with ERBB inhibition alone and this inhibition was increased with the addition of AZ8010 (Fig. 4A, Supplemental Figure 1A). When combinations of AZ8010 and AZD8931 were examined over multiple concentrations, synergistic growth inhibition of UMSCC25 cells (as evidenced by CI indices  $<0.5$ ) was readily apparent (Fig. 4B). Importantly, neither 584-A2 nor CCL30 cells responded to AZD8931 alone (Supplemental Figure 1C) and the drug failed to increase growth inhibition combined with AZ8010 (Fig. 4C). These findings demonstrate the specificity of AZD8931 and are consistent with the identification of ERBB2 as a SLAT only in UMSCC25 cells (Fig. 4B). Similar results were observed with the pan-ERBB inhibitor, lapatinib (Supplemental Figure 5). To investigate whether other HNSCC cell lines would similarly respond to the combination of FGFR and ERBB inhibition, we tested additional HNSCC cell lines that we previously identified as exhibiting dual growth inputs through ERBB family members and FGFR (Marshall et al., 2011). As shown in Figure 4D, UMSCC1 and UMSCC8 cells showed a greater growth inhibition with combined AZ8010 and AZD8931 relative to either inhibitor alone. To confirm that the effect of AZD8931 was due to inhibition of ERBB family members, ERBB2 was knocked down with two independent shRNAs in UMSCC1 and UMSCC8 cells (Supplemental Figure 6A-C). A similar effect was seen with the combination of ERBB2 knockdown and AZ8010 treatment, suggesting that the targeting of EGFR in addition to other ERBB family members by AZD8931 is partially responsible for the effect. These results show that alternate RTKs such as ERBB2 can

provide protection from FGFR inhibition and that targeting these receptors with a combination of small molecule inhibitors can provide superior cell growth inhibition.

**Combined treatment with FGFR and MET inhibitors synergistically inhibits HNSCC cell line proliferation.** Next, we tested if pharmacologic inhibition of both FGFR and MET, another highly ranked SLAT (Fig. 1B), would yield additive or synergistic growth inhibition in UMSCC25, UMSCC1 and UMSCC8 cells. PF02341066 (PF1066; crizotinib) was originally developed as a MET inhibitor, but has other known targets including anaplastic lymphoma kinase (ALK) (Zou et al., 2007; Kwak et al., 2010). PF1066 blocked phosphorylation of MET in UMSCC25 at concentrations consistent with published data (Supplemental Figure 4B), indicating that MET is basally activated in untreated cells. HNSCC cell lines were treated with PF1066 and AZ8010 alone and in combination in anchorage independent or clonogenic growth assays. We found that PF1066 alone inhibited the growth of UMSCC25 cells, in which MET was identified as a SLAT (Supplemental Figure 1A). Furthermore, AZ8010 alone modestly inhibited the growth of these cells, but enhanced the growth inhibition in combination with PF1066 (Fig. 5A). Over a range of doses, the combination of PF1066 and AZ8010 provoked a synergistic response in the cell line UMSCC25, with maximal synergy observed at higher doses of both drugs (Fig. 5B). To validate the screen results, we tested whether 584-A2 and CCL30 cells, in which MET was not identified as a SLAT, would respond to the combination treatment. 584-A2 cells but not CCL30 cells express MET (Figure 2B). While PF1066 treatment moderately reduced growth of 584-A2 cells and CCL30 cells, the combination treatment of AZ8010 and PF1066 did not increase the effect of AZ8010 on these cells (Fig. 5C, Supplemental Figure 1D). UMSCC1 and

UMSCC8 cells, previously shown to respond to a combination of FGFR and ERBB family member inhibition (Fig. 4D), also showed an enhanced growth inhibition with the combination of FGFR and MET inhibition as compared to the single treatments (Fig. 5D). This effect of PF1066 was validated by knockdown of MET in UMSCC1 and UMSCC8 cells (Supplemental Figure 6D-F). Thus, our results demonstrate that different HNSCC cell lines rely on distinct repertoires of RTKs for growth and survival and their combined inhibition can achieve a superior growth inhibition relative to any one TKI alone.

We have shown that the combination of AZ8010 and AZD8931 or the combination of AZ8010 and PF1066 can synergistically inhibit the clonogenic growth of a subset of HNSCC lines. To assess the mechanism of this growth inhibition, we used immunoblot analysis to measure pERK in extracts from UMSCC25 cells treated with different combinations of the TKIs. We have previously shown that decreased ERK signaling occurs following inhibition of the dominant RTKs in HNSCC cell lines (Marshall et al., 2011). In Figure 6A, either AZ8010 or AZD8931 alone reduce the level of ERK phosphorylation, but the combination treatment provides a nearly complete ablation of ERK phosphorylation (Fig. 6A, columns 1-7). In contrast, PF1066 treatment slightly increased pERK and the addition of AZ8010 lowers levels to control levels (Fig. 6A, columns 1, 8-11). Moreover, inhibition of MET phosphorylation with PF1066 slightly lowered pSTAT3 levels, suggesting MET may be one component of multiple pathways maintaining STAT3 signaling in these cells (Fig. 6A, columns 1, 8-11). We detected no effect of the TKIs on pAKT (Figure 6A).

We tested whether the combination therapies cause a decrease in clonogenic growth through an increase in apoptosis. Levels of cleaved PARP and caspase-3 increase with AZ8931 and PF1066 treatment while the combination of AZ8010 and AZD8931 or the combination of AZ8010 and AZD8931 does not appreciably increase the levels (Fig. 6B). However, AZ8010 and PF1066 combination treatment did increase apoptosis as measured by a caspase-3 activity assay (Fig. 6C). Thus, we find that the two combination treatments function in slightly different manners to decrease clonogenic growth. AZ8010 and AZD8931 combination causes a decrease in proliferation through enhanced inhibition of ERK signaling while the combination of AZ8010 and PF1066 yields a decrease in STAT3 phosphorylation. Both treatments increase in apoptosis although it is unclear if the combination treatments cause significantly more apoptosis than the single treatments.

**The triple combination of AZ8010, AZD8931 and PF1066 strongly inhibits HNSCC cell growth accompanied by induction of apoptosis.** The combined inhibition of FGFR and ERBB2 or MET provides a more complete decrease in growth than inhibition of one RTK. We postulated that UMSCC25, UMSCC1 and UMSCC8 depend on EGFR, ERBB2, MET and FGFR for maximal growth, and inhibition of all four RTKs would be required to achieve maximal growth inhibition. UMSCC25, UMSCC1 and UMSCC8 cells were treated with AZ8010, AZD8931 and PF1066 alone, with the three distinct combinations of two inhibitors and with a combination of all three inhibitors, and the effects on clonogenic growth were measured. As shown in Figure 7A, the triple combination resulted in a significantly greater inhibition of growth relative to any of the double combinations. To determine whether the triple combination was

exerting a non-specific cytotoxic effect on the cells, we treated MSK-921 HNSCC cells in the same manner. MSK-921 cells are highly and exclusively dependent on EGFR (data not shown). As expected, the cell line only exhibited a decrease in anchorage dependent growth when treated with the pan-ERBB inhibitor, AZD8931, with no evidence of additive effects with FGFR or MET inhibition (Fig. 7B). Likewise, growth of the highly FGFR dependent cell lines, 584-A2 and CCL30, was inhibited by AZ8010 with no evidence of additive effects by other TKIs (Fig. 7C). Importantly, the triple treatment lead to a significant induction in apoptosis as measured by PARP and caspase-3 cleavage (Fig. 6B) or caspase-3 activity (Fig. 6C). These results indicate a subset of HNSCC cell lines engage multiple RTKs for growth and survival signaling and that simultaneous inhibition of multiple receptors is necessary to maximally inhibit growth.

## **Discussion:**

Our results show that coactivation of RTK networks is critical for maintenance of growth and survival in a subset of HNSCC cell lines. Research has already identified a role for EGFR as a driver of growth in HNSCC tumors, leading to the approval of cetuximab for the treatment of the disease (Specenier et al., 2011). Also, ERBB2 and MET have both been found to be overexpressed in HNSCC and *in vitro* experiments have indicated a role for these receptors as mediators of HNSCC growth (Morgan et al., 2009; Seiwert et al., 2009). This work shows that RTKs have the ability to function as a network such that effective growth inhibition requires their simultaneous blockade.

Recent research is unveiling the general importance of RTK networks in cancer and the relevance to cancer cell response to targeted therapy. For example, glioblastoma cell lines and primary tumors show activation of multiple RTKs. While a dominant RTK preferentially drives downstream signaling, a secondary RTK can maintain signaling through the pathway when the dominant RTK is inhibited (Huang et al., 2007; Stommel et al., 2007). Additionally, in breast cancer cells resistant to the ERBB2 inhibiting antibody, trastuzumab, cells maintain growth and survival signaling through ERBB2, ERBB3 and insulin-like growth factor-I receptor (IGF-IR) heterotrimers that are formed exclusively in the resistant cells (Huang et al., 2010). Evidence from cell lines and primary tumor samples indicate that coactivation of multiple RTKs also functions in ovarian cancer (Jiao et al., 2011) and gastric cancer (Kataoka et al., 2011). Proposed mechanisms to target these RTK networks include inhibitor combinations, multitargeted inhibitors or inhibition of common downstream signaling components (Xu et al., 2010).

Our results raise significant questions about the strategies previously used to identify targets in HNSCC. Clearly, the search for effective targeted therapies for HNSCC has been hampered by the general lack of oncogenic mutations that characterize the cancer type (Agrawal et al., 2011; Stransky et al., 2011). In fact, researchers have speculated whether the disease may, in fact, be untreatable using targeted therapies and that clinical progress can only occur through improved prevention and early detection (Agrawal et al., 2011). However, combined with observations that many cell lines respond with growth inhibition to EGFR inhibitors (Marshall et al., 2011), but tumors do not respond well to the same therapy in the clinic, these data may instead imply that non-mutational changes in the cell, such as coactivation of RTKs, are driving growth. A coupling of disruption of tumor suppressors such as p53 or p16 and the coactivation of multiple RTKs to maintain pro-growth and anti-apoptosis signaling robustness could be proposed to be driving tumorigenesis in, if not all, then a large proportion of HNSCC tumors. Thus, we propose that developing approaches to identify and target non-mutated oncogene driver pathways and networks in HNSCC is critical for significant therapeutic advances in this cancer.

The question remains how to effectively and efficiently determine the subtype into which a particular HNSCC cell line will reside with the ultimate goal of identifying the most appropriate therapy approach for each individual patient. Our present study shows that a subset of HNSCC cell lines do respond to combined inhibition of multiple RTKs while other cell lines seem to be highly dependent on a single RTK (Figure 7). It has been suggested that a method to overcome the robustness of a RTK network is to target a shared, downstream signaling protein (Xu et al., 2010). This strategy would



negate the need to individually tailor treatments to the specific network activated in a particular tumor. Unfortunately, we did not find a shared node downstream of the different RTKs in the three cell lines that were screened (Figure 1, Supplemental Table 2). To fully understand the heterogeneity of HNSCC, more cell lines would need to be screened, but these results suggest that downstream targets would also be subject to the drawbacks of targeting receptors. One of the strengths of an unbiased, functional screen is that it can identify pathways or genes crucial to the growth of the cancer cell that are not mutated or otherwise deregulated. Growing evidence indicates these sort of drivers are present in cancer and will be missed by more traditional screening methods such as large scale sequencing (Luo et al., 2009). Unfortunately, while these pathways and genes may have vital roles and can be targeted clinically, by their very nature, they do not lend themselves to straightforward screening methods, such as SNaPshot (Sequist et al., 2011). Therefore, work is needed to develop tractable biomarkers for proper patient selection. It is conceivable that individual RNAi screens could be deployed in cell lines developed from each patient's tumor in order to design a rational, personalized treatment regime.

The findings from our study provide *in vitro*, preclinical support for combinations of TKIs as a superior therapeutic approach to managing HNSCC. In this regard, the recent review by Glickman and Sawyers provides a compelling argument for therapy with rationally-defined combinations of targeted drugs that induce synergistic killing of cancer cells relative to the transient responses observed with monotherapies as both a practical and necessary step in the evolution of modern cancer therapeutics (Glickman et al., 2012). Their argument is based on the clear successes with combination

therapies in the management of HIV and tuberculosis infections in humans where monotherapies provide only transient responses. As many small molecule inhibitors of RTKs are in various stages of clinical development, targeting multiple RTKs in the clinic with combinations of inhibitors is a feasible goal, albeit with technical and logistic hurdles as well.

**Authorship Contributions:**

Participated in research design: Singleton, Casás-Selves, DeGregori, and Heasley.

Conducted experiments: Singleton, Hinz, Marek, and Hatheway.

Data analysis: Singleton, Kim, Tan, and Heasley.

Wrote and contributed to manuscript: Singleton, Kim, Tan, and Heasley.

## References:

- Agrawal N, Frederick MJ, Pickering CR, Bettgowda C, Chang K, Li RJ, Fakhry C, Xie TX, Zhang J, Wang J, Zhang N, El-Naggar AK, Jasser SA, Weinstein JN, Trevino L, Drummond JA, Muzny DM, Wu Y, Wood LD, Hruban RH, Westra WH, Koch WM, Califano JA, Gibbs RA, Sidransky D, Vogelstein B, Velculescu VE, Papadopoulos N, Wheeler DA, Kinzler KW and Myers JN (2011). Exome sequencing of head and neck squamous cell carcinoma reveals inactivating mutations in NOTCH1. *Science* **333**: 1154-1157.
- Ang KK, Andratschke NH and Milas L (2004). Epidermal growth factor receptor and response of head-and-neck carcinoma to therapy. *Int J Radiat Oncol Biol Phys* **58**: 959-965.
- Casas-Selves M, Kim J, Zhang Z, Helfrich BA, Gao D, Porter CC, Scarborough HA, Bunn PA, Jr., Chan DC, Tan AC and Degregori J (2012). Tankyrase and the canonical Wnt pathway protect lung cancer cells from EGFR inhibition. *Cancer Res*.
- Cecchi F, Rabe DC and Bottaro DP (2010). Targeting the HGF/Met signalling pathway in cancer. *Eur J Cancer* **46**: 1260-1270.
- Cohen EE (2006). Role of epidermal growth factor receptor pathway-targeted therapy in patients with recurrent and/or metastatic squamous cell carcinoma of the head and neck. *J Clin Oncol* **24**: 2659-2665.
- Cohen EE, Rosen F, Stadler WM, Recant W, Stenson K, Huo D and Vokes EE (2003). Phase II trial of ZD1839 in recurrent or metastatic squamous cell carcinoma of the head and neck. *J Clin Oncol* **21**: 1980-1987.
- Dassonville O, Formento JL, Francoual M, Ramaioli A, Santini J, Schneider M, Demard F and Milano G (1993). Expression of epidermal growth factor receptor and survival in upper aerodigestive tract cancer. *J Clin Oncol* **11**: 1873-1878.
- Druker BJ (2002). Perspectives on the development of a molecularly targeted agent. *Cancer Cell* **1**: 31-36.
- Egloff AM and Grandis JR (2009). Improving Response Rates to EGFR-Targeted Therapies for Head and Neck Squamous Cell Carcinoma: Candidate Predictive Biomarkers and Combination Treatment with Src Inhibitors. *J Oncol* **2009**: 896407.
- Gazdar AF (2009). Activating and resistance mutations of EGFR in non-small-cell lung cancer: role in clinical response to EGFR tyrosine kinase inhibitors. *Oncogene* **28 Suppl 1**: S24-31.
- Glickman MS and Sawyers CL (2012). Converting cancer therapies into cures: lessons from infectious diseases. *Cell* **148**: 1089-1098.
- Grandis JR, Melhem MF, Barnes EL and Twardy DJ (1996). Quantitative immunohistochemical analysis of transforming growth factor-alpha and epidermal growth factor receptor in patients with squamous cell carcinoma of the head and neck. *Cancer* **78**: 1284-1292.
- Grandis JR, Melhem MF, Gooding WE, Day R, Holst VA, Wagener MM, Drenning SD and Twardy DJ (1998). Levels of TGF-alpha and EGFR protein in head and neck squamous cell carcinoma and patient survival. *J Natl Cancer Inst* **90**: 824-832.

- Haddad RI and Shin DM (2008). Recent advances in head and neck cancer. *N Engl J Med* **359**: 1143-1154.
- Hickinson DM, Klinowska T, Speake G, Vincent J, Trigwell C, Anderton J, Beck S, Marshall G, Davenport S, Callis R, Mills E, Grosios K, Smith P, Barlaam B, Wilkinson RW and Ogilvie D (2010). AZD8931, an equipotent, reversible inhibitor of signaling by epidermal growth factor receptor, ERBB2 (HER2), and ERBB3: a unique agent for simultaneous ERBB receptor blockade in cancer. *Clin Cancer Res* **16**: 1159-1169.
- Hopkins AL and Groom CR (2002). The druggable genome. *Nat Rev Drug Discov* **1**: 727-730.
- Huang PH, Mukasa A, Bonavia R, Flynn RA, Brewer ZE, Cavenee WK, Furnari FB and White FM (2007). Quantitative analysis of EGFRvIII cellular signaling networks reveals a combinatorial therapeutic strategy for glioblastoma. *Proc Natl Acad Sci U S A* **104**: 12867-12872.
- Huang X, Gao L, Wang S, McManaman JL, Thor AD, Yang X, Esteva FJ and Liu B (2010). Heterotrimerization of the growth factor receptors erbB2, erbB3, and insulin-like growth factor-i receptor in breast cancer cells resistant to herceptin. *Cancer Res* **70**: 1204-1214.
- Hynes NE and Lane HA (2005). ERBB receptors and cancer: the complexity of targeted inhibitors. *Nat Rev Cancer* **5**: 341-354.
- Jiao Y, Ou W, Meng F, Zhou H and Wang A (2011). Targeting HSP90 in ovarian cancers with multiple receptor tyrosine kinase coactivation. *Mol Cancer* **10**: 125.
- Kalyankrishna S and Grandis JR (2006). Epidermal growth factor receptor biology in head and neck cancer. *J Clin Oncol* **24**: 2666-2672.
- Kataoka Y, Mukohara T, Tomioka H, Funakoshi Y, Kiyota N, Fujiwara Y, Yashiro M, Hirakawa K, Hirai M and Minami H (2011). Foretinib (GSK1363089), a multi-kinase inhibitor of MET and VEGFRs, inhibits growth of gastric cancer cell lines by blocking inter-receptor tyrosine kinase networks. *Invest New Drugs*.
- Kim J and Tan AC (2012). BiNGS!SL-seq: a bioinformatics pipeline for the analysis and interpretation of deep sequencing genome-wide synthetic lethal screen. *Methods Mol Biol* **802**: 389-398.
- Kwak EL, Bang YJ, Camidge DR, Shaw AT, Solomon B, Maki RG, Ou SH, Dezube BJ, Janne PA, Costa DB, Varella-Garcia M, Kim WH, Lynch TJ, Fidias P, Stubbs H, Engelman JA, Sequist LV, Tan W, Gandhi L, Mino-Kenudson M, Wei GC, Shreeve SM, Ratain MJ, Settleman J, Christensen JG, Haber DA, Wilner K, Salgia R, Shapiro GI, Clark JW and Iafrate AJ (2010). Anaplastic lymphoma kinase inhibition in non-small-cell lung cancer. *N Engl J Med* **363**: 1693-1703.
- Ladanyi M and Pao W (2008). Lung adenocarcinoma: guiding EGFR-targeted therapy and beyond. *Mod Pathol* **21 Suppl 2**: S16-22.
- Leemans CR, Braakhuis BJ and Brakenhoff RH (2011). The molecular biology of head and neck cancer. *Nat Rev Cancer* **11**: 9-22.
- Licitra L, Mesia R, Rivera F, Remenar E, Hitt R, Erfan J, Rottey S, Kaweckki A, Zabolotnyy D, Benasso M, Storkel S, Senger S, Stroh C and Vermorken JB (2011). Evaluation of EGFR gene copy number as a predictive biomarker for the efficacy of cetuximab in combination with chemotherapy in the first-line treatment

- of recurrent and/or metastatic squamous cell carcinoma of the head and neck: EXTREME study. *Ann Oncol* **22**: 1078-1087.
- Luo J, Solimini NL and Elledge SJ (2009). Principles of cancer therapy: oncogene and non-oncogene addiction. *Cell* **136**: 823-837.
- Marshall ME, Hinz TK, Kono SA, Singleton KR, Bichon B, Ware KE, Marek L, Frederick BA, Raben D and Heasley LE (2011). Fibroblast growth factor receptors are components of autocrine signaling networks in head and neck squamous cell carcinoma cells. *Clin Cancer Res* **17**: 5016-5025.
- Matassa AA, Carpenter L, Biden TJ, Humphries MJ and Reyland ME (2001). PKCdelta is required for mitochondrial-dependent apoptosis in salivary epithelial cells. *J Biol Chem* **276**: 29719-29728.
- Morgan S and Grandis JR (2009). ErbB receptors in the biology and pathology of the aerodigestive tract. *Exp Cell Res* **315**: 572-582.
- Morse DL and Gillies RJ (2010). Molecular imaging and targeted therapies. *Biochem Pharmacol* **80**: 731-738.
- Murdoch D (2007). Standard, and novel cytotoxic and molecular-targeted, therapies for HNSCC: an evidence-based review. *Curr Opin Oncol* **19**: 216-221.
- O'Dwyer ME, Mauro MJ, Blasdel C, Farnsworth M, Kurilik G, Hsieh YC, Mori M and Druker BJ (2004). Clonal evolution and lack of cytogenetic response are adverse prognostic factors for hematologic relapse of chronic phase CML patients treated with imatinib mesylate. *Blood* **103**: 451-455.
- Perou CM, Sorlie T, Eisen MB, van de Rijn M, Jeffrey SS, Rees CA, Pollack JR, Ross DT, Johnsen H, Akslen LA, Fluge O, Pergamenschikov A, Williams C, Zhu SX, Lonning PE, Borresen-Dale AL, Brown PO and Botstein D (2000). Molecular portraits of human breast tumours. *Nature* **406**: 747-752.
- Porter CC, Kim J, Fosmire S, Gearheart CM, van Linden A, Baturin D, Zaberezhnyy V, Patel PR, Gao D, Tan AC and Degregori J (2012). Integrated genomic analyses identify WEE1 as a critical mediator of cell fate and a novel therapeutic target in acute myeloid leukemia. *Leukemia* **26**: 1266-1276.
- Robinson MD and Smyth GK (2007). Moderated statistical tests for assessing differences in tag abundance. *Bioinformatics* **23**: 2881-2887.
- Sato-Kuwabara Y, Neves JI, Fregnani JH, Sallum RA and Soares FA (2009). Evaluation of gene amplification and protein expression of HER-2/neu in esophageal squamous cell carcinoma using Fluorescence in situ Hybridization (FISH) and immunohistochemistry. *BMC Cancer* **9**: 6.
- Seiwert TY, Jagadeeswaran R, Faoro L, Janamanchi V, Nallasura V, El Dinali M, Yala S, Kanteti R, Cohen EE, Lingen MW, Martin L, Krishnaswamy S, Klein-Szanto A, Christensen JG, Vokes EE and Salgia R (2009). The MET receptor tyrosine kinase is a potential novel therapeutic target for head and neck squamous cell carcinoma. *Cancer Res* **69**: 3021-3031.
- Sequist LV, Heist RS, Shaw AT, Fidias P, Rosovsky R, Temel JS, Lennes IT, Digumarthy S, Waltman BA, Bast E, Tammireddy S, Morrissey L, Muzikansky A, Goldberg SB, Gainor J, Channick CL, Wain JC, Gaissert H, Donahue DM, Muniappan A, Wright C, Willers H, Mathisen DJ, Choi NC, Baselga J, Lynch TJ, Ellisen LW, Mino-Kenudson M, Lanuti M, Borger DR, Iafrate AJ, Engelman JA

- and Dias-Santagata D (2011). Implementing multiplexed genotyping of non-small-cell lung cancers into routine clinical practice. *Ann Oncol* **22**: 2616-2624.
- Shepherd FA, Rodrigues Pereira J, Ciuleanu T, Tan EH, Hirsh V, Thongprasert S, Campos D, Maoleekoonpiroj S, Smylie M, Martins R, van Kooten M, Dediu M, Findlay B, Tu D, Johnston D, Bezjak A, Clark G, Santabarbara P and Seymour L (2005). Erlotinib in previously treated non-small-cell lung cancer. *N Engl J Med* **353**: 123-132.
- Soulieres D, Senzer NN, Vokes EE, Hidalgo M, Agarwala SS and Siu LL (2004). Multicenter phase II study of erlotinib, an oral epidermal growth factor receptor tyrosine kinase inhibitor, in patients with recurrent or metastatic squamous cell cancer of the head and neck. *J Clin Oncol* **22**: 77-85.
- Specenier P and Vermorken JB (2011). Cetuximab in the treatment of squamous cell carcinoma of the head and neck. *Expert Rev Anticancer Ther* **11**: 511-524.
- Stambuk S, Sundov D, Kuret S, Beljan R and Andelinovic S (2010). Future perspectives of personalized oncology. *Coll Antropol* **34**: 763-769.
- Stommel JM, Kimmelman AC, Ying H, Nabioullin R, Ponugoti AH, Wiedemeyer R, Stegh AH, Bradner JE, Ligon KL, Brennan C, Chin L and DePinho RA (2007). Coactivation of receptor tyrosine kinases affects the response of tumor cells to targeted therapies. *Science* **318**: 287-290.
- Stransky N, Egloff AM, Tward AD, Kostic AD, Cibulskis K, Sivachenko A, Kryukov GV, Lawrence MS, Sougnez C, McKenna A, Shefler E, Ramos AH, Stojanov P, Carter SL, Voet D, Cortes ML, Auclair D, Berger MF, Saksena G, Guiducci C, Onofrio RC, Parkin M, Romkes M, Weissfeld JL, Seethala RR, Wang L, Rangel-Escareno C, Fernandez-Lopez JC, Hidalgo-Miranda A, Melendez-Zajgla J, Winckler W, Ardlie K, Gabriel SB, Meyerson M, Lander ES, Getz G, Golub TR, Garraway LA and Grandis JR (2011). The mutational landscape of head and neck squamous cell carcinoma. *Science* **333**: 1157-1160.
- Sullivan KD, Padilla-Just N, Henry RE, Porter CC, Kim J, Tentler JJ, Eckhardt SG, Tan AC, Degregori J and Espinosa JM (2012). ATM and MET kinases are synthetic lethal with nongenotoxic activation of p53. *Nat Chem Biol*.
- Whitlock MC (2005). Combining probability from independent tests: the weighted Z-method is superior to Fisher's approach. *J Evol Biol* **18**: 1368-1373.
- Xu AM and Huang PH (2010). Receptor tyrosine kinase coactivation networks in cancer. *Cancer Res* **70**: 3857-3860.
- Zou HY, Li Q, Lee JH, Arango ME, McDonnell SR, Yamazaki S, Koudriakova TB, Alton G, Cui JJ, Kung PP, Nambu MD, Los G, Bender SL, Mroczkowski B and Christensen JG (2007). An orally available small-molecule inhibitor of c-Met, PF-2341066, exhibits cytoreductive antitumor efficacy through antiproliferative and antiangiogenic mechanisms. *Cancer Res* **67**: 4408-4417.

**Footnotes:**

The studies were supported by a National Institutes of Health grant [R01 CA127105].



## **Figure Legends:**

**FIGURE 1: Synthetic lethal interactions with FGFR inhibition are identified using a genome-wide RNAi-based loss-of-function screen. A)** As described in the Materials and Methods, the HNSCC cell lines UMSCC25, CCL30 and 584-A2 were transduced with a genome-wide shRNA library and either treated with the FGFR inhibitor, AZ8010 or DMSO control for 72 hours. After recovering for an additional 72 hours, RNA was isolated from the cells and nested PCR was performed to isolate the shRNA sequences and to add Illumina adaptor sequences. Samples were submitted to Illumina sequencing and the reads were analyzed by BiNGS! **B)** Tabular representation of the shRNA counts obtained by deep sequencing for the ten most highly ranked SLATs in UMSCC25 cells as well as ERBB2. The intensity of red indicates the number of shRNA read counts in each replicate for both the control and AZ8010 treated groups. Each line corresponds to an independent shRNA targeting the indicated gene. The top ten hits and the data for ERBB2 for UMSCC25 cells are shown. **C)** Synthetic lethal hits (SLATs) ( $E$  value  $\leq 20$ ) among growth receptors and their common downstream signaling pathways. SLATs identified in the UMSCC25 cells are shaded red, SLATs in 584-A2 cells are shaded green, and SLATs in CCL30 cells are shaded blue. Pathway members that were not identified as SLATs in any cell line are unshaded. The number listed near each SLAT is the p-value (see Materials and Methods).

**FIGURE 2: A panel of HNSCC cell lines shows variable expression of ERBB2 and MET protein.** Whole cell lysates of the indicated HNSCC cell lines were collected and

immunoblotted for **A)** ERBB2 or **B)** MET. Filters were stripped and reprobed for the  $\alpha$ -subunit of Na/K ATPase as a loading control.

**FIGURE3: Confirmation of ERBB2 and MET as synthetic lethal genes with FGFR inhibition by targeted knockdown. A)** Pooled UMSCC25 cells expressing either a negative control shRNA targeting GFP or two independent shRNAs targeting either ERBB2 or MET were generated and ERBB2 or MET protein expression was measured by immunoblotting. The protein level of the  $\alpha$ -subunit of Na/K-ATPase was measured as a loading control. **B)** Pooled UMSCC25 cells expressing the control shRNA or one of two shRNAs targeting ERBB2 were used in a clonogenic growth assay in the presence or absence of 1.0  $\mu$ M AZ8010. After two weeks, colonies were stained and quantified as described in the Materials and Methods. **C)** Pooled UMSCC25 cells expressing the control shRNA or one of two shRNAs targeting MET were used in a clonogenic growth assay in the presence or absence of 1.0  $\mu$ M AZ8010. After two weeks, colonies were stained and quantified as described in the Materials and Methods. The data are the means and SEM of three replicates from three independent experiments; ns indicates not significant, \* indicates  $p < 0.05$  and \*\* indicates  $p < 0.005$  using a two-tailed Student's t-test.

**FIGURE 4: Combined inhibition of ERBB family members and FGFR leads to synergistic impairment of the growth of HNSCC cell lines. A)** UMSCC25 cells were treated in triplicate with DMSO, 3.0 nM AZD8931 or 10 nM AZD8931 alone or in combination with 0.5  $\mu$ M AZ8010 or 1.0  $\mu$ M AZ8010. The effect of the treatments on cell

growth was measured by clonogenic assay. **B)** UMSCC25 cells were plated in triplicate and treated with DMSO, AZ8010, AZD8931 and the combinations at the doses shown. Proliferation was measured after one week by the CyQuant assay as described in the Materials and Methods and plotted on the top chart. Data are the means of two independent experiments. Combination Indices (CI) were calculated using the Calcsyn program and shown on the bottom table where the strength of the synergism is indicated by the darkness of shading. **C)** As in A, except 584-A2 cells were treated with DMSO, 30 nM AZD8931, 30 nM AZ8010 and the combination. CCL30 cells were treated with DMSO, 100 nM AZD8931, 100 nM AZ8010 and the combination. The growth of 584-A2 cells was measured by clonogenic assay and the growth of CCL30 cells was measured using an anchorage independent growth assay as described in the Materials and Methods. **D)** As in A, except UMSCC1 and UMSCC8 cells were treated with DMSO, 30 nM AZD8931, 30 nM AZ8010 and the combination. Data are the means and SEM of three independent experiments. Statistical analysis using a two-tailed Student's t-test showed significant differences in clonogenic growth where ns indicates not significant, \* indicates  $p < 0.05$ , \*\* indicates  $p < 0.005$  and \*\*\*\* indicates  $p < 0.0001$ .

**FIGURE 5: Combined inhibition of MET and FGFR leads to synergistic impairment of the growth of HNSCC cell lines. A)** UMSCC25 cells were treated in triplicate with DMSO, 0.1  $\mu$ M PF1066 or 0.5  $\mu$ M PF1066 alone or in combination with 0.5  $\mu$ M AZ8010 or 1.0  $\mu$ M AZ8010. The effect of the treatments on cell growth was measured by clonogenic assay. **B)** UMSCC25 cells were plated in triplicate and treated with DMSO, AZ8010, PF1066 and the combinations at the doses shown. Proliferation was measured

by CyQuant assay as described in the Materials and Methods and plotted on the top chart. Data are the means of two independent experiments. Combination Indices (CI) were calculated and shown on the bottom table. **C)** As in A, except 584-A2 cells were treated with DMSO, 0.5  $\mu$ M PF1066, 30 nM AZ8010 and the combination and growth was measured by clonogenic assay. CCL30 cells were treated with DMSO, 0.3  $\mu$ M PF1066, 0.1  $\mu$ M AZ8010 and the combination and growth was measured by anchorage independent growth assay. **D)** As in A, except UMSCC1 and UMSCC8 cells were treated with DMSO, 0.3  $\mu$ M PF1066, 0.3  $\mu$ M AZ8010 and the combination and growth was measured by clonogenic assay. Data are the means and SEM of three independent experiments. Statistical analysis using a two-tailed Student's t-test was used to show significant differences in growth where ns indicates not significant, \* indicates  $p < 0.05$ , \*\* indicates  $p < 0.005$ , \*\*\* indicates  $p < 0.0005$  and \*\*\*\* indicates  $p < 0.0001$ .

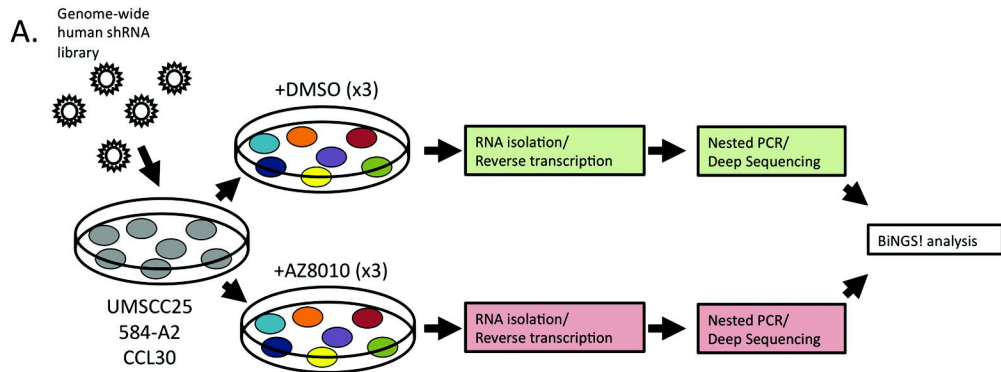
**FIGURE 6: Effects of combined FGFR, ERBB family and MET inhibition on ERK signaling and PARP cleavage. A)** UMSCC25 cells were treated with the indicated doses ( $\mu$ M) of DMSO, AZ8010, AZD8931 or PF1066 alone and in combination for 6 hours in full media. Extracts were prepared and proteins resolved by SDS-PAGE. The filters were immunoblotted for pERK, pSTAT3 and pAKT. The filters were then stripped and reprobed for total ERK1/2, total STAT3, total AKT and the  $\alpha$ -subunit of NA/K ATPase as a loading control. **B)** UMSCC25 cells were treated as with the drugs indicated in **A)** with the doses ( $\mu$ M) shown for 72 hours. Extracts were prepared and proteins resolved by SDS-PAGE. The filters were immunoblotted for PARP. The filters were then stripped and reprobed for the  $\alpha$ -subunit of NA/K ATPase as a loading control.

**C)** UMSCC25 cells were treated as described in **B)** and caspase activity was measured as described in the Materials and Methods.

**FIGURE 7: Simultaneous inhibition of FGFR, ERBB family receptors and MET**

**leads to greater growth inhibition compared to the double combinations in a subset of HNSCC cell lines. A)** UMSCC25, UMSCC1 and UMSCC25 were treated in triplicate with 0.5  $\mu$ M AZ8010, 10 nM AZD8931, 0.1  $\mu$ M PF1066, the respective double combinations and the triple combination. Growth was measured by clonogenic assay and quantified after 2 weeks. **B)** MSK-921 cells were treated in triplicate as in A. Growth was measured via anchorage independent growth assay. **C)** 584-A2 cells were treated in triplicate with 0.1  $\mu$ M AZ8010, 10 nM AZD8931, 0.1  $\mu$ M PF1066, the respective double combinations and the triple combination. Growth was measured after 2 weeks by clonogenic assay. CCL30 cells were treated in triplicate with 0.1  $\mu$ M AZ8010, 10 nM AZD8931, 0.1  $\mu$ M PF1066, the respective double combinations and the triple combination. Growth was measured after 2 weeks using an anchorage independent growth assay. Data are the means and SEM of three independent experiments. Statistical analysis using a two-tailed Student's t-test revealed significant differences in growth where ns indicates not significant, \* indicates  $p < 0.05$ , \*\* indicates  $p < 0.005$ , \*\*\* indicates  $p < 0.0005$  and \*\*\*\* indicates  $p < 0.0001$ .

# Figure 1



**B.**

Rank	Gene Name	shRNA	DMSO			AZ12908010		
1	CLUAP1	54885	286	350	336	197	300	154
		54895	27	3	7	0	0	0
		54891	45	4	91	7	0	2
		54890	0	26	49	8	0	0
		44124	17	2	13	1	0	0
2	ZFR	211698	15	8	9	0	0	0
		88001	5	4	1	1	0	0
		44122	80	124	77	34	66	73
		44125	1084	653	1987	563	712	761
		81676	13	56	0	0	0	0
3	MET	90022	43	19	24	0	3	11
		89986	31	8	180	0	7	9
		110205	0	34	70	0	0	0
4	MEMO1	18775	0	31	73	0	0	0
		81614	9	62	127	5	3	0
		81611	6	3	109	0	2	0
5	NPAT	81613	0	4	2	0	1	0
		129052	99	0	159	8	0	0
		127371	994	57	202	2	18	44
7	G2E3	126708	0	38	1916	0	0	0
		126696	7	6	2	0	0	0
		126702	173	3	52	0	32	0
8	PSMD13	41644	11	13	11	0	0	0
		41648	0	8	4	2	0	3
		41646	3	38	4	0	0	0
		102370	1	0	25	0	0	0
9	MUC7	99679	47	6	782	13	0	10
		99682	6	6	2	4	4	2
		67550	1108	928	1155	604	1095	721
10	ARSD	162507	11	9	12	0	0	0
		63819	2	33	0	0	0	0
		79425	36	4	111	0	0	0
82	ERBB2	79425	36	4	111	0	0	0

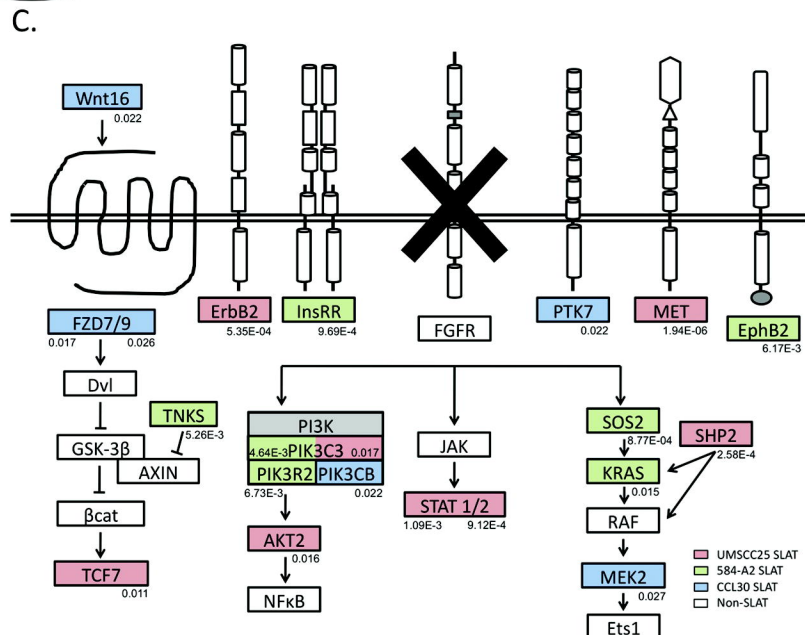
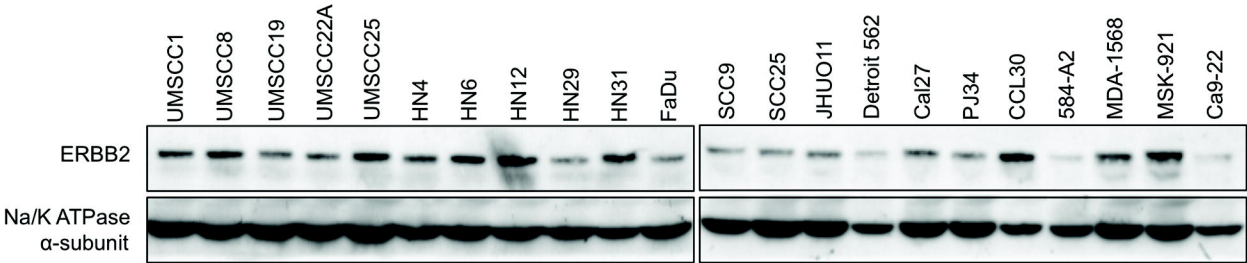


Figure 2

A.



B.

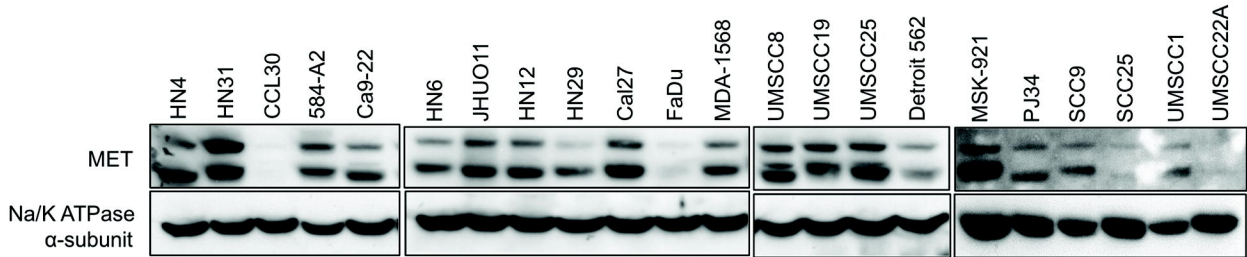
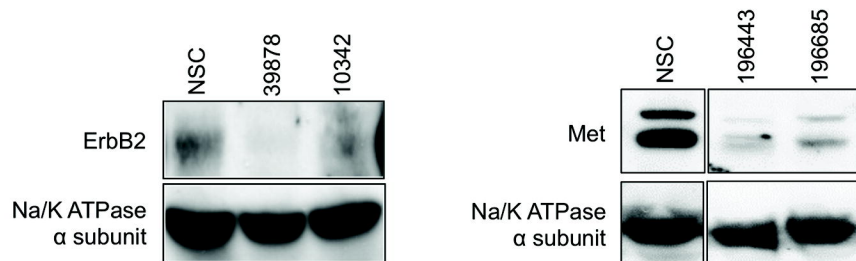
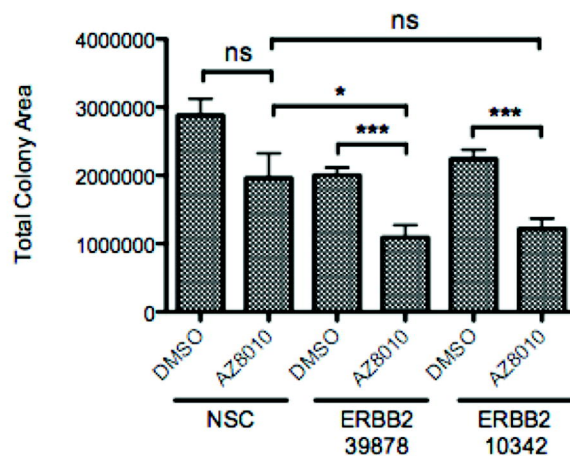


Figure 3

A.



B.



C.

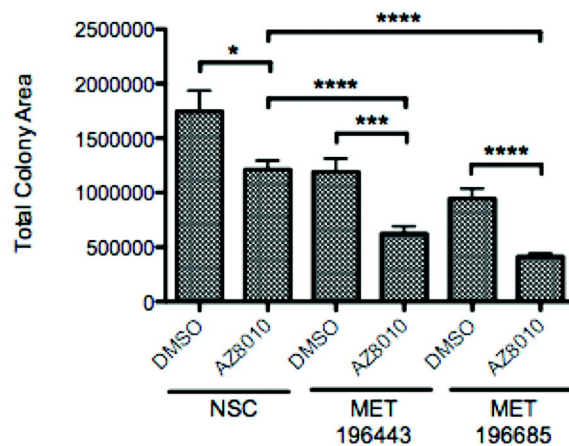
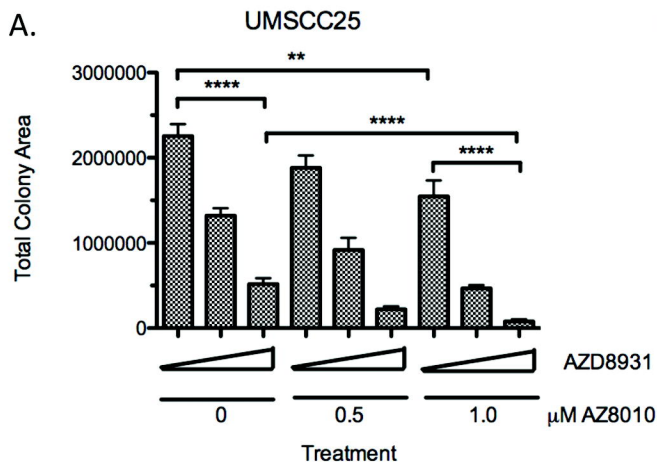


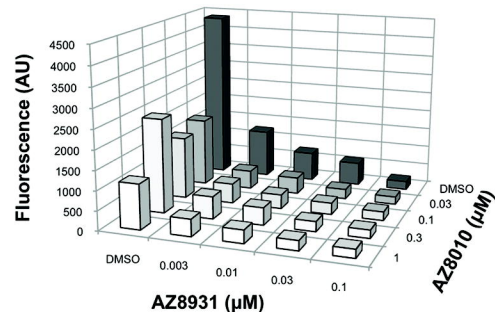


# Figure 4

A.



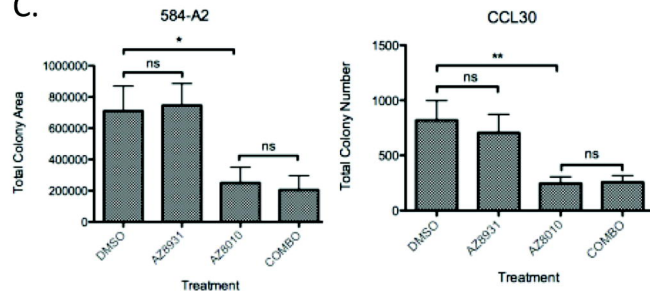
B.



		AZ8931 (μM)			
		0.003	0.01	0.03	0.1
AZ8010 (μM)	1.0	0.095	0.188	0.312	0.799
	0.3	0.17	0.33	0.332	0.744
	0.1	0.129	0.216	0.429	0.828
	0.03	0.112	0.295	0.312	0.639

Synergism: Very Strong Strong Synergism Moderate

C.



D.

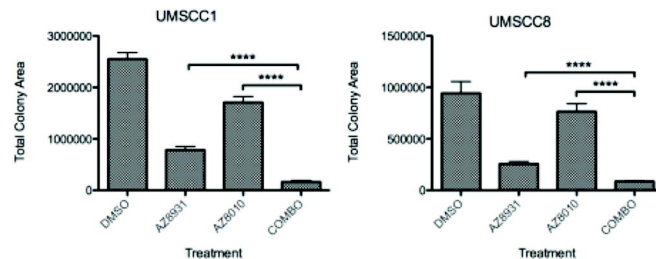
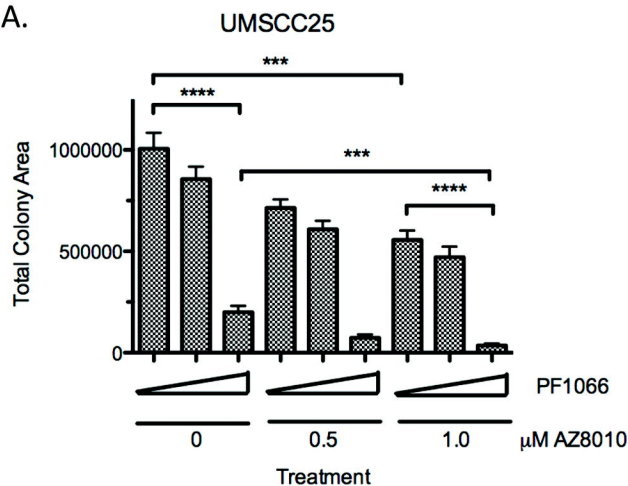
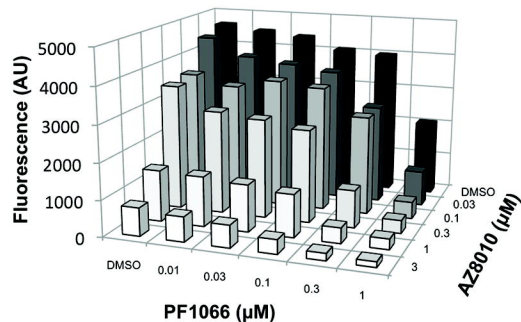


Figure 5

A.



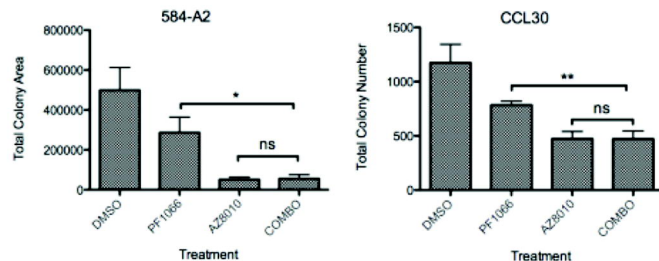
B.



		PF1066 (μM)				
		0.01	0.03	0.1	0.3	1.0
AZ8010 (μM)	3.0	0.912	0.805	0.485	0.227	0.175
	1.0	0.756	0.696	0.618	0.185	0.131
	0.3	0.190	0.067	0.889	0.821	0.765
	0.1	0.708	0.482	0.822	0.594	0.053
	0.03	0.387	0.415	0.618	0.409	0.125

Synergism: Very Strong Strong Synergism Moderate Additive

C.



D.

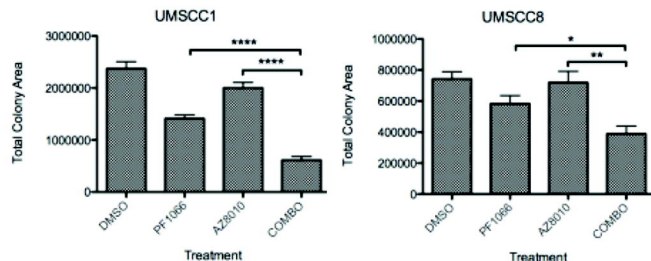


Figure 6

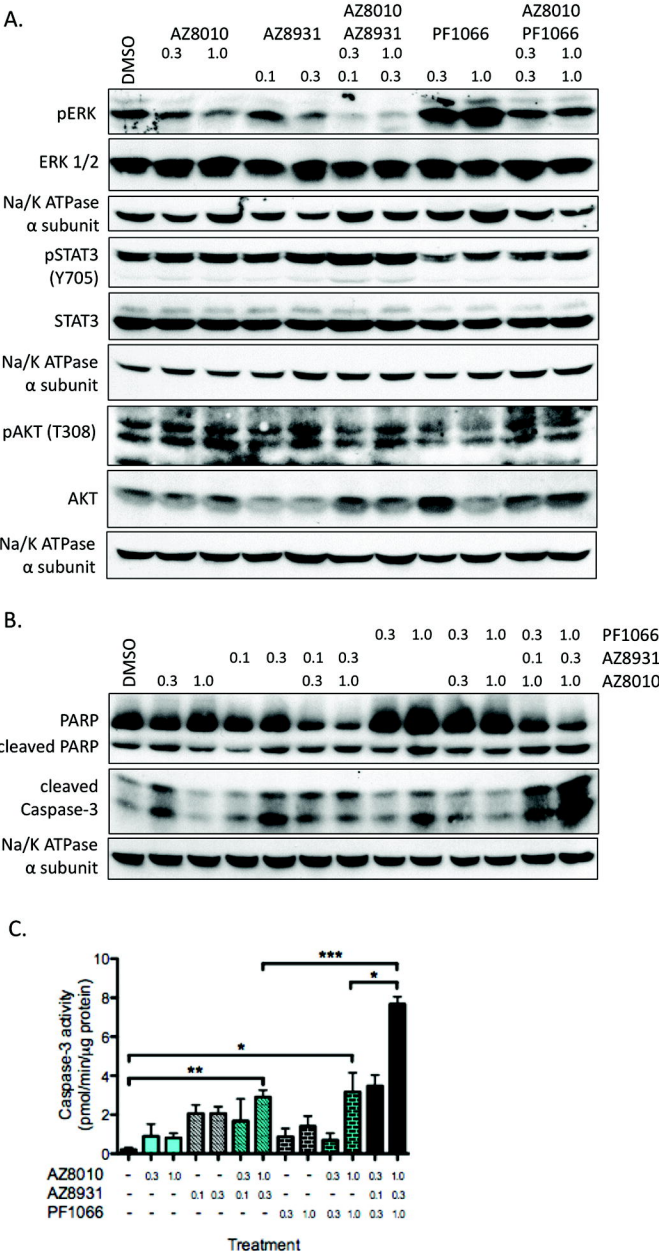


Figure 7

